Facies analysis and diagenetic evolution of the Dinantian carbonates in the Dutch subsurface: data and analyses well LTG-01

Report by SCAN

October 2019

Ministerie van Economische Zaken en Klimaat
ebn
TNO
Interreg North-West Europe DGE-ROLLOUT

Facies analysis and diagenetic evolution of the Dinantian carbonates in the Dutch subsurface: data and analyses well LTG-01

Written by:
Mahtab Mozafari[1], Peter Gutteridge[2], Alberto Riva[3], Kees Geel[4], Joanna Garland[2] and Julie Dewit[2]

October 2019

1- Energie Beheer Nederland (EBN), Daalsesingel 1, 3511 SV Utrecht, the Netherlands
2- Cambridge Carbonates Ltd, No. 4 The Courtyard, 707 Warwick Road, Solihull, B91 3DA, UK
3- G.E.Plan Consulting srl, Via L. Ariosto 58, 44121 Ferrara, Italy
4- Geological Survey of the Netherlands (TNO), Princetonlaan 6, 3584 CB Utrecht, the Netherlands

Dit rapport is een product van het SCAN-programma en wordt mogelijk gemaakt door het Ministerie van Economische Zaken en Klimaat

Table of contents

8. Luttelgeest-01 (LTG-01)

8.1 Introduction

The Luttelgeest-01 well is located in the North Central Netherlands (Figure 8-1, Table 8-1), drilled close to the Emmeloord-01 well (EMO-1). Drilling started on 26th May 2004, and the well was abandoned on 8 March 2005, with gas shows.

The well encountered a thick Visean section (768 m), overlying Famennian clastics. The Dinantian was the primary target. The LTG-01 well is located on the Luttelgeest carbonate platform which is found on the Texel-IJsselmeer structural high, a prominent NW-SE trending fault block of mid-Palaeozoic origin (Lipsey et al., 2016). The southern boundary is made up of a steep fault system, while the northern margin gradually transitions into the adjacent Friesland platform. The Luttelgeest carbonate platform is elongated in the E-W direction, with dimensions of approximately 14 km E-W and 8 km N-S. Figures 8-2 and 8-3 shows the seismic interpretation and morphology of the Luttelgeest platform by Van Hulten and Poty (2009).

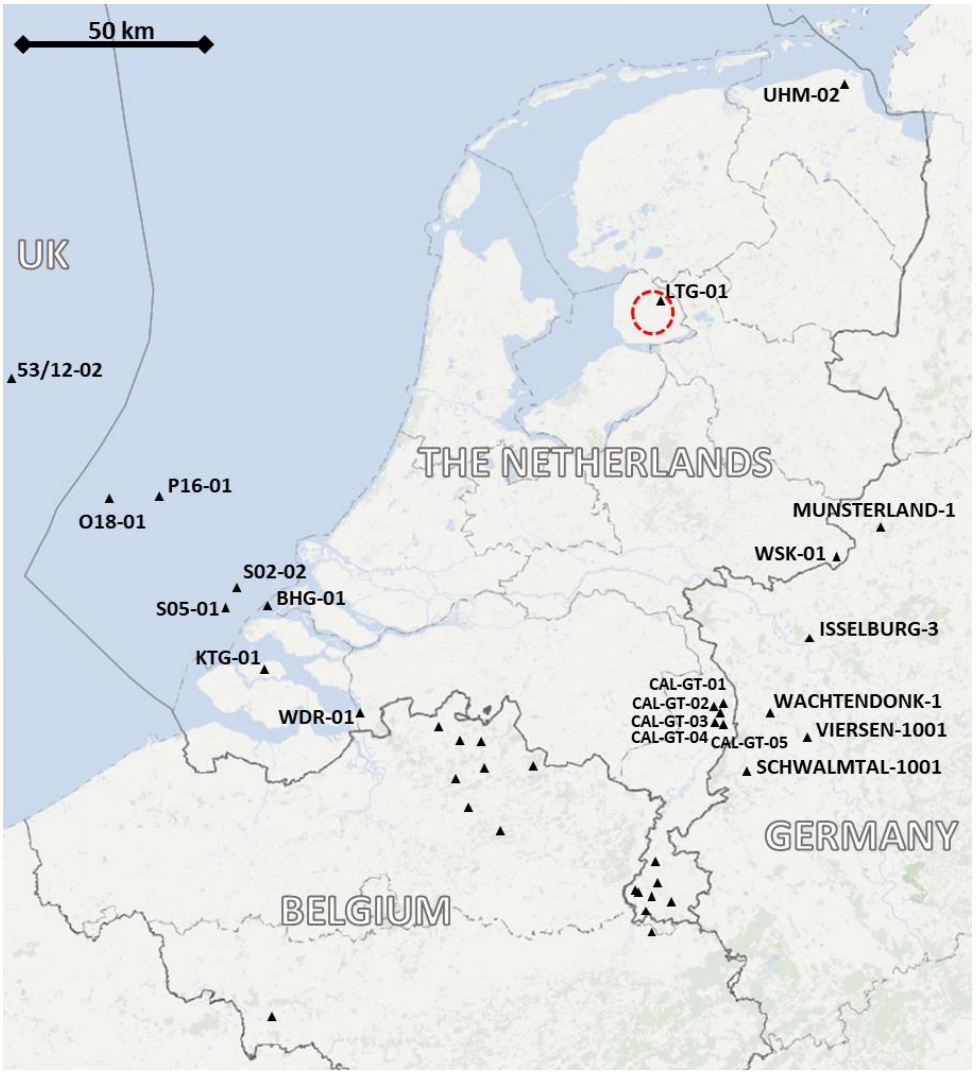

Figure 8-1: Map showing all the wells penetrating the Dinantian carbonates. Location of the LTG-01 well is indicated by a red dashed circle.

Table 8-1: Coordinates and depth of LTG-01 well.

Co-ordinates (x, y in utm31, ed50 format)	689328 , 5844373
Lat/Long (°)	52.71497777, 5.80288113
Supplied co-ordinates	183003.6, 525283.4 (RD)
Depth in meters referred to :	Rotary Table
Total depth (m, along hole) :	5162
Vertical position of Rotary Table :	5.86 meter relative to NAP
Trajectory shape :	Deviated
Deviation in X-direction :	210.83
Deviation in Y-direction :	-302.76
True vertical depth (TVD) in m :	5115.742

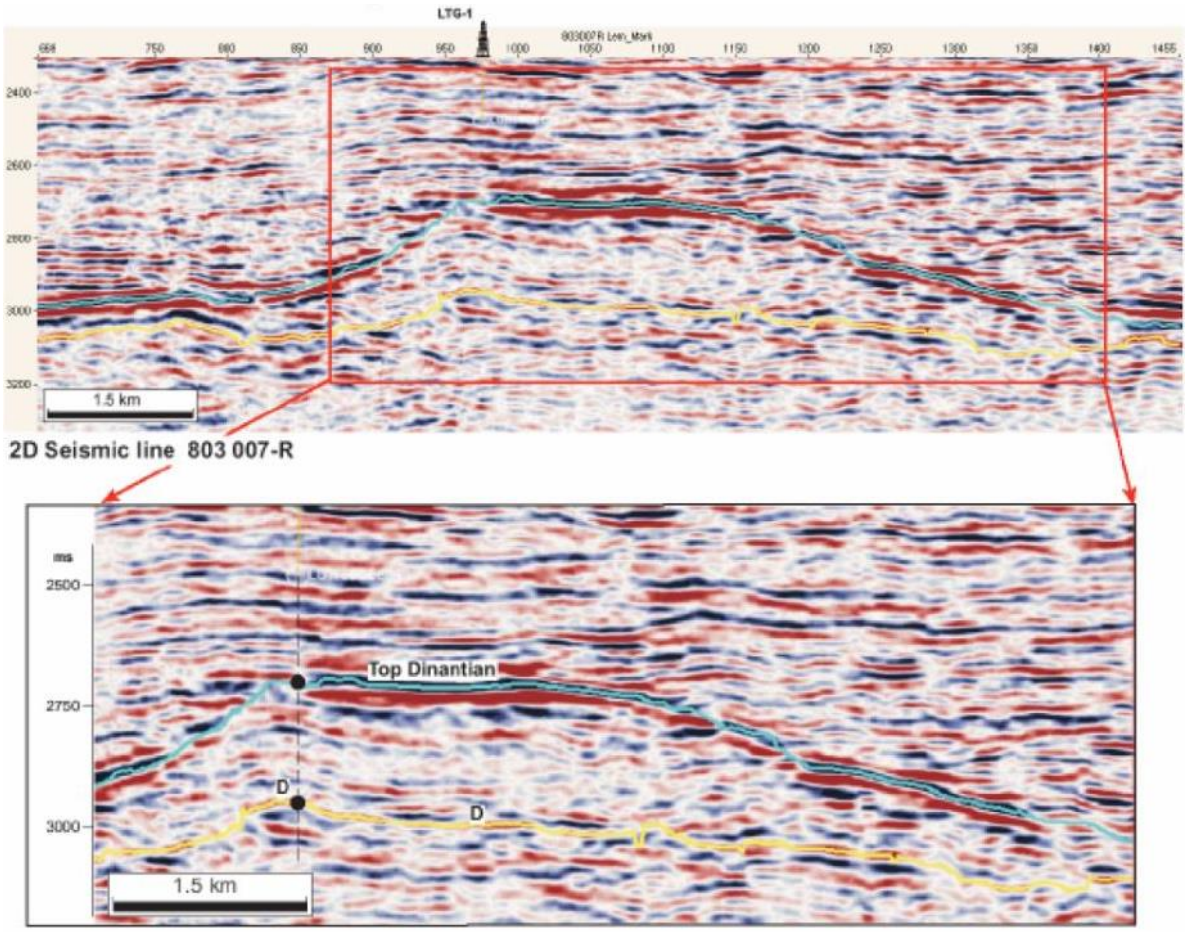

Figure 8-2: Interpretation (line 803007R) of the Luttelgeest carbonate platform by Van Hulten and Poty (2009).

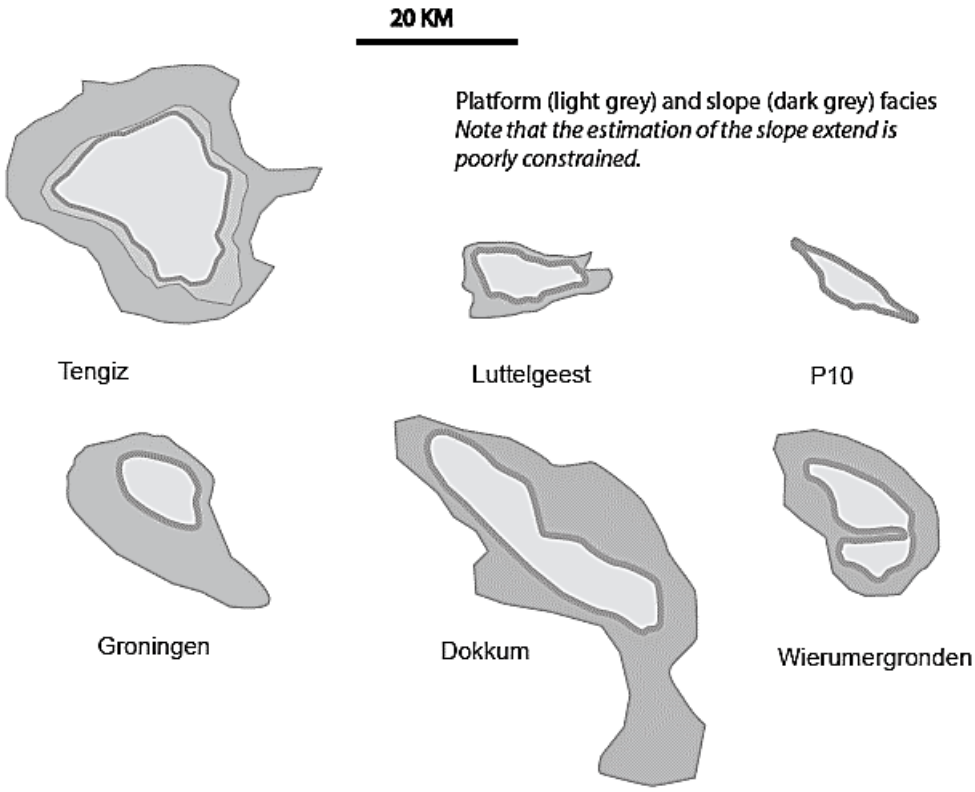

Figure 8-3: Comparison between Luttelgeest platform and other Carboniferous carbonate platforms around the world (From Van Hulten, 2012)

8.2 Available dataset

Most of the available data and reports on the LTG-01 well are available on "www.nlog.nl" with the following link:

https://www.nlog.nl/nlog/requestData/nlogp/allBor/metaData.jsp?tableName=BorLocation&id=106532593

Boxem, T. A. P., Veldkamp, J. G., and van Wees, J. D. A. M. (2016). Ultra-diepe geothermie: Overzicht, inzicht and to-do ondergrond. TNO 2016 R10803 Eindrapport, 53, 1-53.

Goldberg, A. T., Millan, I., Lipsey, L., and Nelskamp, S. (2017). Geothermal exploration in deep Dinantian carbonates in the Netherlands. Utrecht.

Hoornveld, N. (2013). Dinantian carbonate development and related prospectivity of the onshore. Vrije Universiteit Amsterdam.

Lipsey, L., van Wees, J.-D., and Pluymaekers, M. P. D. (2015). Numerical Modelling of Thermal Convection Related to Fracture Permeability-Implications for Geothermal Exploration and Basin Modelling. In First EAGE/TNO Workshop Basin Hydrodynamic Systems in Relations to their Contained Resources, Utrecht, 5 p.

Lipsey, L., Pluymaekers, M., Goldberg, T., Van Oversteeg, K., Ghazaryan, L., Cloetingh, S., and van Wees, J. D. (2016). Numerical modelling of thermal convection in the Luttelgeest carbonate platform, the Netherlands. Geothermics, 64, 135-151. https://doi.org/10.1016/j.geothermics.2016.05.002

Lokhorst, A., and Van Wees, J.-D. (2005). NITG 05-068-B0510 Technical and economical feasibility of a Deep Borehole Heat Exchanger (DBHE) in LTG-01, Utrecht.

Ter Heege, J. H., Osinga, S., and Carpentier, S. (2018). The Geomechanical Response of Naturally Fractured Carbonate Reservoirs to Operation of a Geothermal Doublet. 52nd U.S. Rock Mechanics/Geomechanics Symposium, 791, 13 p.

Total (2004). Final drilling and completion report. 143 p.

Total (2004). LTG-01 Composite Log.

Total (2005). Final Report Testing and Abandonment Luttelgeest 1 (LTG01). 12 p.

Total (2005). Core photos and core measurements. 5p.

Vachard (2004). Cuttings descriptions LTG-01. 5p.

Van Hulten, F. F. N. (2012). Devono-carboniferous carbonate platform systems of the Netherlands. Geologica Belgica, 15, 284-296.

Van Hulten, F. F. N., and Poty, E. (2009). Dinantian Reefs underneath the Netherlands. In 71st EAGE Conference and Exhibition, Amsterdam, 4 p.

Van Leverink, D., and Geel, C.R. (2019). Fracture characterization of the Dinantian Carbonates in the Dutch Subsurface. SCAN Report. Report downloadable from www.nlog.nl/scan.

Van Oversteeg, K., Lipsey, L., Pluymaekers, M., Van Wees, J. D., and Fokker, P. A. (2014). Fracture Permeability Assessment in Deeply Buried Carbonates and Implications for Enhanced Geothermal Systems: Inferences from a Detailed Well Study at Luttelgeest-01, The Netherlands. In Proceedings of 39th Stanford Geothermal Workshop.

8.2.1 Logs

A full suite of logs is available for a complete petrophysics re-evaluation within the framework of the SCAN project (Figure 8-4). The LTG-01 well does not encounter any clay in the Dinantian interval.

8.2.2 Cores, sidewall cores and cuttings

Two short cores were cut in the Dinantian intervals. Core 1 from 4378.5 to 4376 m, and core 2 from 4473 m to 4470 m. No sidewall cores were taken.

8.2.3 Thin sections

A total number of 16 cuttings thin sections and nine core thin sections were made available by TNO. These thin sections were photographed and briefly described. A full description of cuttings thin sections is also available in Goldberg et al. (2017) (Table 8-2 and Figure 8-8).

8.2.4 Additional analyses

No samples were analysed further for CL, fluid inclusions or geochemistry during the current project. Fluid inclusion data are reported in Van Hulten and Poty (2009) which is just general results rather than a thorough overview. Clumped isotope analysis is performed by Goldberg et al. (2017).

8.3 Sedimentology

Two short cores from near the top of the Dinantian intervals were provided (Figures 8-5 and 8-6). Cores are dominated by bioclastic peloidal packstone and grainstones with abundant crinoids and fragments of echinoids, calcareous algae, foraminifera and brachiopods (Figures 8-7). Locally, bioclasts are aligned. These were deposited in high energy, shallow-water settings, above wave-base. The diverse faunal assemblage suggests a fully open marine setting.

The vast majority of the cuttings are characterised by grain-support, high energy facies. Coated grains and intraclasts are common, suggesting persistent high energy. The microbial nature of many of the cuttings suggest very shallow conditions, and fenestral textures may indicate short-lived exposure (intertidal settings). Siliciclastic cuttings are present but are likely to represent cavings. Dolomite is rare but present towards the base of the well. In the lower 120 m of the well, dolomite is intercalated with limestone. The high API-peaks seen in the gamma ray tool represent Uranium peaks, and do not have any clay content (no Potassium from the spectral GR log). This is similar to the lower parts of the Uithuizermeeden platform. It is possible that the higher Uranium peaks represent calcrete intervals at cycle tops.

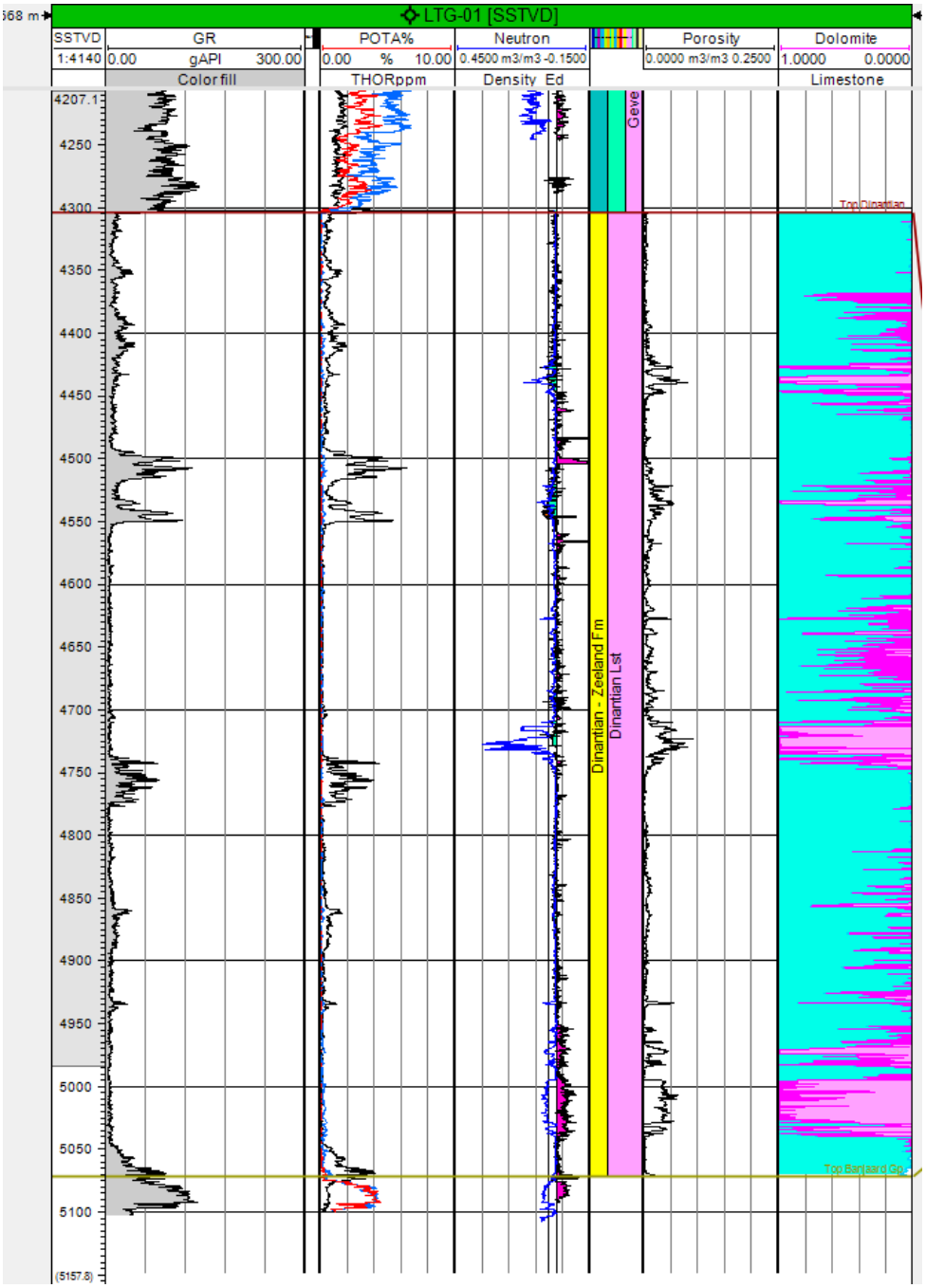

Figure 8-4: Gamma ray, neutron/density, porosity and mineralogical logs in the LTG-01 well.

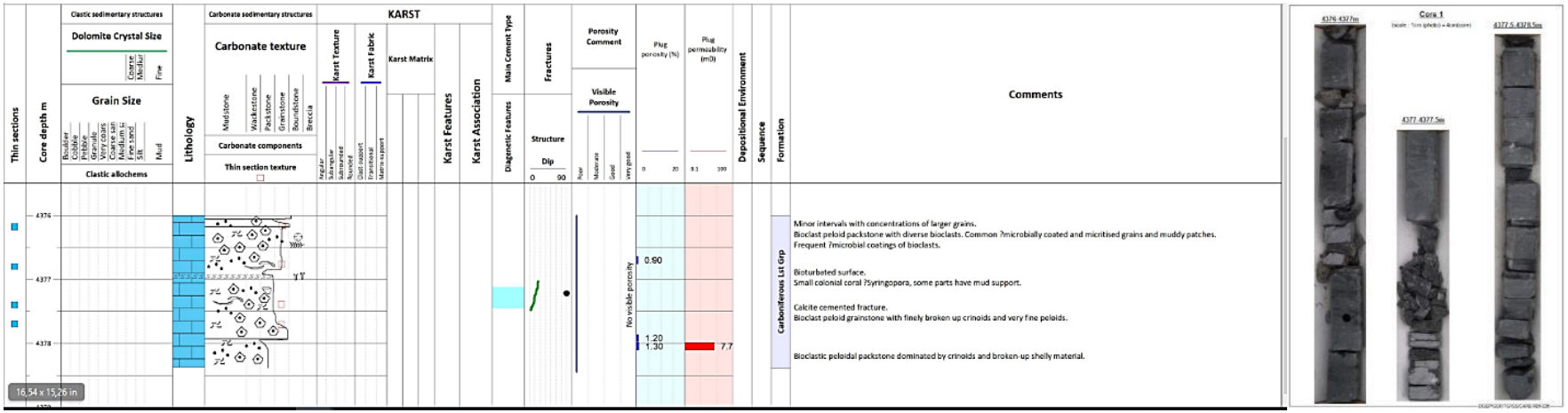

Figure 8-5: Sedimentological description of Core 1. (an image of higher resolution is available in Appendix B as a supplementary document).

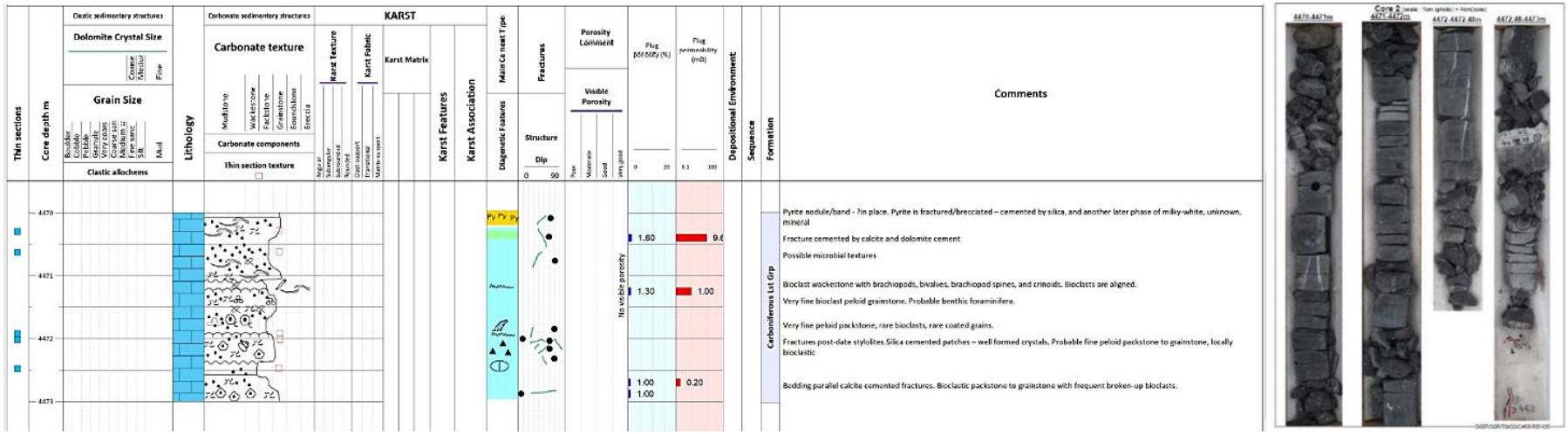

Figure 8-6: Sedimentological description of Core 2. (an image of higher resolution is available in Appendix B as a supplementary document).

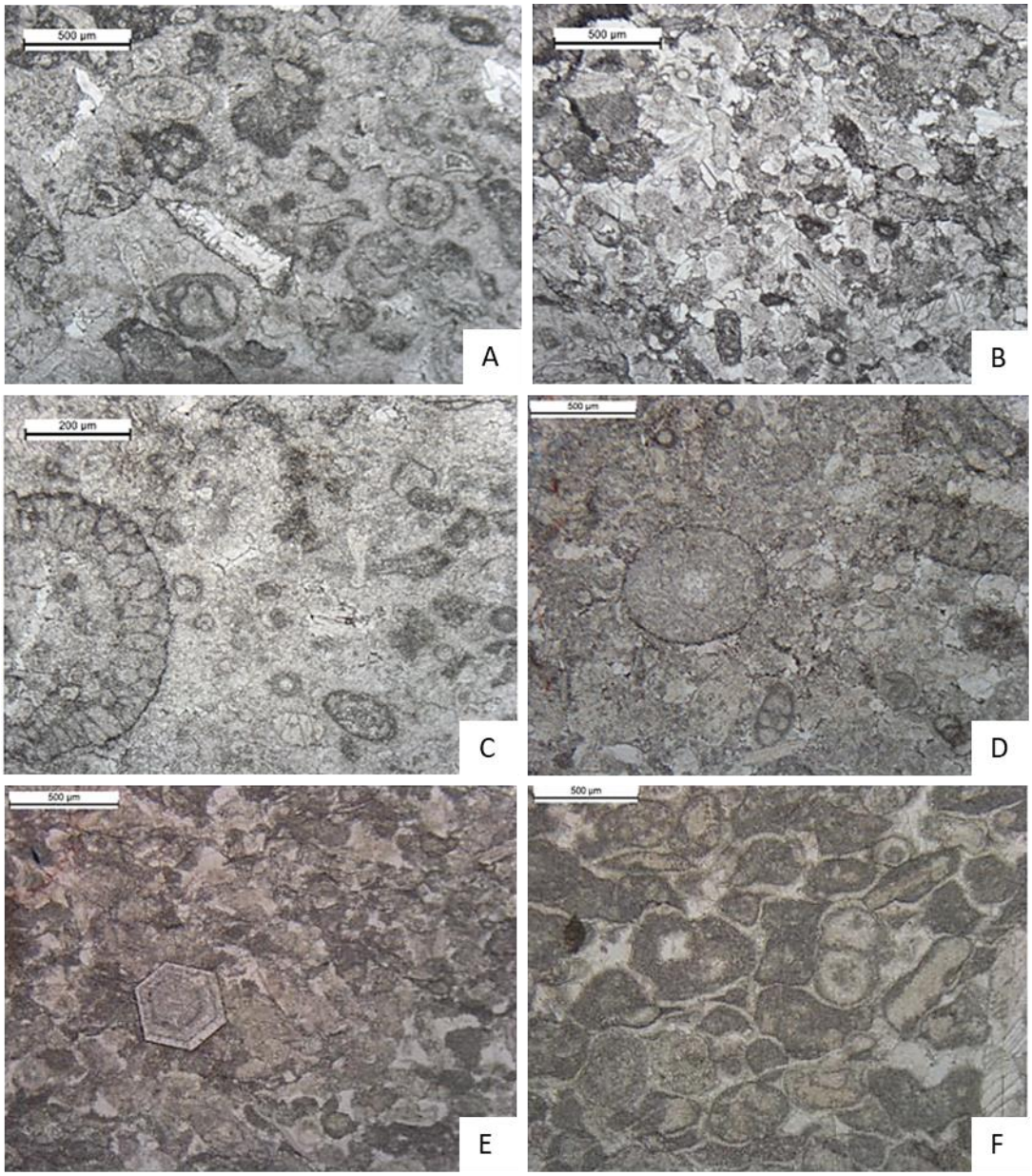

Figure 8-7: Representetive photomicrographs showing the bioclastic grainstones/packstones in LTG-01 well (SCAN project). A, B) Bioclastic grainstone (4376.15 m and 4376.80 m). C) Bioclastic grainstone (4377.40 m). D) Bioclastic packstone (4377.70 m). E) Peloidal-bioclastic grainstone (4470.63 m). F) Peloidal/intraclast-bioclastic grainstone (4472.02 m).

Table 8-2: Summary of the cuttings fragments identified in the LGT-01. From Goldberg et al. (2017).

Depth (m)	Dominant Microfacies*	Microfacies in decreasing order of abundance					Porosity/diagenesis observations
4400	Packstone	Calcite crystals	Fissile shale	Authigenic Quartz			Calcite spar. No visible porosity.
4426	Grainstone/packstone	Sandstone	Calcite crystals	Brecciated frag. (?)	Black fragments	Fissile shale	Large number of clay and siltstone fragments. It is not clear whether this represents caved lithology or original content. No porosity.
4520	Packstone/grainstone	Black fragments	Fissile shale	Pyrite			Siltstone fragments containing mica, clay, heavy minerals and organic particles. Claystone (shale) fragments and siltstones both contain significant disseminated amounts of pyrite. The pyrite was formed at a very early stage, before significant compaction, possibly from to anoxic pore-water generation.
4570	Grainstone	Packstone	Black fragments	Sandstone	Saddle dolomite	Fissile shale	Calcite crystals: These fragments comprise calcite spar that may be derived from either fracture infills or calcite replacement (Plate 10). Siltstones are interlayered with carbonate. Some chalcedony is present.
4600	Grainstone/packstone	Calcite crystals	Black fragments	Fissile shale	Saddle Dolomite		Fissile shale consists of laminated black silty shale with layers of carbonaceous siltstone heavily compacted flaser clay (partly authigenic) and mica (Plate 11). This might represent a caved fragment.
4650	Grainstone	Dolomite (saddle)	Authigenic quartz				Less siliciclastic components than in previous two cuttings samples. Minor saddle dolomite and non-ferroan dolomite. No visible porosity. Authigenic quartz.
4768	Packstone	Calcite crystal					-
4800	Grainstone	Packstone	Sandstone				-
4902	Packstone/Grainstone						Siltstones are interlayered with carbonate. Some chalcedony is present. Some recrystallisation.
4946	Packstone/Grainstone	Fissile shale					Several carbonate fragments contain large (ca. 1mm) calcite sparite fill, which could be indicative of karstification.
5010	Packstone/Grainstone	Dolomite crystals	Authigenic quartz				Some saddle dolomite is present.

5052	Packstone	Dolomite crystals	Grainstone	Wackestone with calcispheres			Large increase in dolomite (ca. 40%). The sample contains both common dolomite spar, as well as saddle dolomite. The baroque dolomite is present as fracture fill and as intergranular pore fill and replacement of calcite. Euhedral pyrite (trace) in carbonate. Dolomite is post calcite spar. Some brecciated material. Possibly early brecciation and subsequent cementation. Trace authigenic quartz. Some of the saddle dolomites fragments contain intergranular pores (plate 12, A, examples arrowed).
5066	Saddle dolomite	Sandstone	Authigenic Quartz	Brecciated Cc and Dol crystals			Ca. 50% dolomite, non-ferroan and baroque dolomite Layers of carbonaceous siltstone. Heavily compacted with flaser clay (partly authigenic) and mica. The shale is heavily compacted. Siltstones contain fractures filled with quartz and ferroan dolomite. The ferroan dolomite postdates quartz and non-ferroan dolomite. The detrital components of the siltstones are overgrown with authigenic microquartz (Plate 13). The siltstone is partially cemented with dolomite. Baroque dolomite (d) is intergrown with the siltstone quartz representing a late stage recrystallization of (probably) carbonate or a fracture fill. Authigenic quartz (q) crystallised prior to dolomite. Potential primary karstic feature.
5082	Grainstone/packstone	Dolomite crystals					Dolomite content decreases again to less than 15%.

*****Cutting samples might present a bias at the time of collecting fine and coarse cutting at the same location.

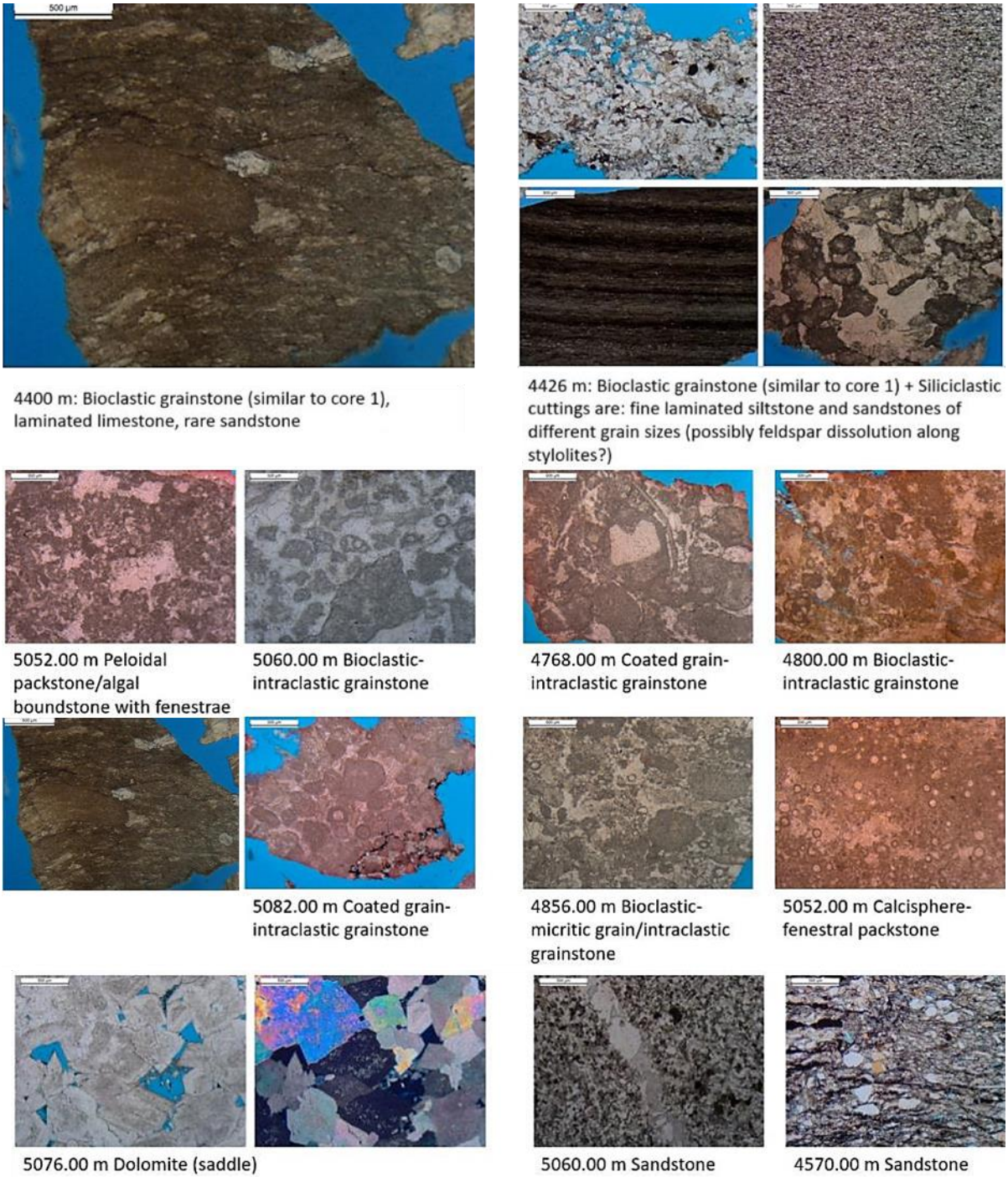

Figure 8-8: Different microfacies encountered in the LTG-01 well.

8.4 Stratigraphy

The intervals encountered by the LTG-01 well span from Quaternary to Devonian. The Cretaceous unconformity was found at 1727 m MD and the Top Dinantian is at 4355 m.

Table 8-3: Stratigraphic succession of the LTG-01 well (from www.nlog.nl).

Stratigraphical unit	Top interval	Base interval
Upper North Sea Gp.	0	480
Lower North Sea Gp.	480	760
Brussels Sand Mb.	760	840
Ieper Mb.	840	1043
Landen Fm.	1043	1105
Ommelanden Fm.	1105	1576
Texel Fm.	1576	1643
Lower Holland Marl Mb.	1643	1721
Vlieland Claystone Fm.	1721	1727
Slochteren Fm.	1727	1776
Ruurlo Fm.	1776	1911
Baarlo Fm.	1911	2788
Geul Subgroep	2788	3022
Ubachsberg Mb.	3022	3237
Epen Fm.	3237	4132
Geverik Mb.	4132	4355
Carboniferous Limestone Gp.	4355	5123
Banjaard Gp.	5123	5162

8.5 Biostratigraphy

The only biostratigraphic data available is that of Vachard (2004), based on cuttings. Only the uppermost 150 m of the carbonate succession was analysed, and many of the samples could not be dated. Three samples suggest the following ages (Table 8-4):

Depth (m)	Zone
4376	Livian; V2b/V3a
4464	Molinacian (Chadian-Arundian); Cf4α/ɣ
4470	Late Molinacian (Arundian); V2a/ Cf4ɣ (OR Cf6 (RC7α), from Van Hulten and Poty (2009) – see comment below)

The age of Livian near the top of the carbonate interval suggests that the entire Warnantian (Asbian-Brigantian) is missing in the well – either not deposited, or eroded/karstified. Van Hulten and Poty (2009) also note that biostratigraphy indicates a major hiatus between the Namurian and the lower Visean of the carbonates. The faunas have been checked, and whilst a Livian (Holkerian) age cannot be confirmed for 4376m, a V2a age is still considered to be correct for *Plectogyranopsis* at 4464 m. Somewhat confusingly, Van Hulten and Poty (2009) also comment that the cored interval at 4470.48 m show an association of corals that can be dated as lowermost Cf6 (RC7α), but this is considerably younger than the Cf4ɣ age attributed to the same depth by Vachard (2004).

Whether the absence of Warnantian (Brigantian-Asbian) is due to karstification at the top of the platform is speculative since no indication can be seen on the logs (unless there is no

remnant porosity remaining). Seismic images are only 2D and thus not sufficient to determine if the upper interval is karstified. Petrography indicates that there may be some meteoric cements in the cuttings and intervals of dissolution/collapse which have now been cemented; but this could as easily represent shorter-term 4th order exposures within the carbonate interval. Some mud losses were encountered approx. 90 m below the top carbonate. However, it is noted from the seismic (Figure 8-9) that the well penetrates the side of the isolated platform, and it is possible that the well did not encounter the younger part of the stratigraphy seen in the center of the platform. Based on correlation with the UHM-02 well, the Dinantian succession is thicker at LTG-01, sedimentation rates must therefore have been higher on the Luttelgeest platform during the early Molinacian (Chadian) to Livian (Holkerian). The Warnantian (Asbian-Brigantian) section in LTG-01 may be represented as a highly condensed slope facies.

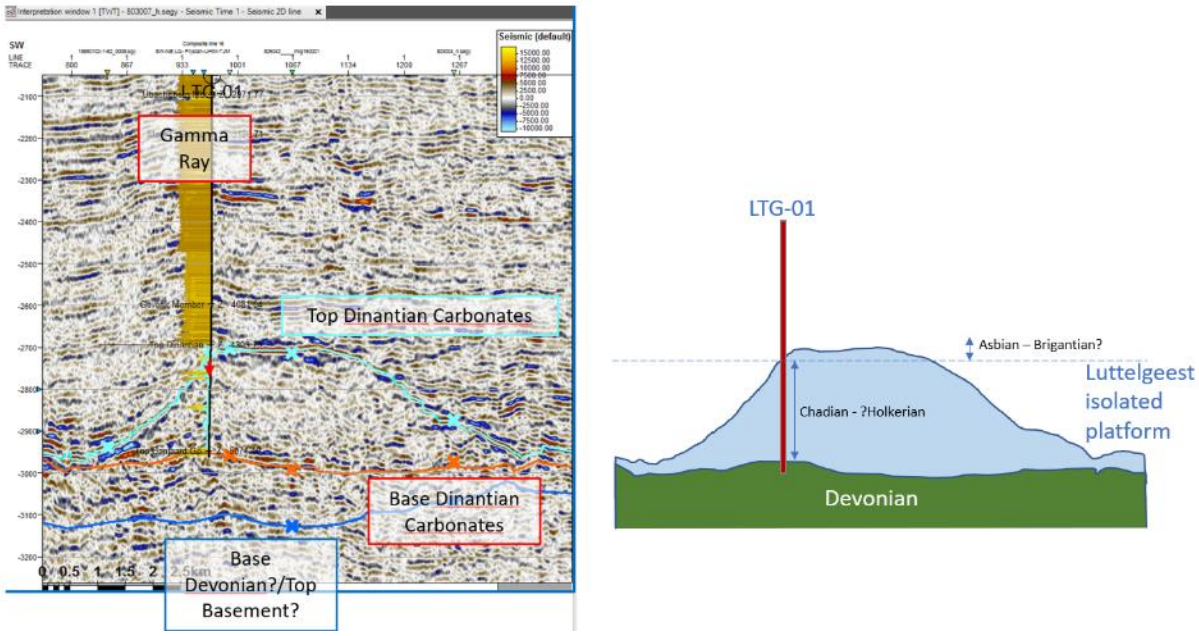

Figure 8-9: Interpreted structure of the Luttelgeest platform.

The lowermost part of the carbonate package has not been dated, so it cannot be confirmed if the Tournaisian is present. From the Vachard (2004) report, there is one genus of foram mentioned which could be Tournaisian in age – Granuliferella (?) sp.; however the identification appears uncertain, and if true would have been reworked. Van Hulten (2012) did not consider any Tournaisian interval when correlating the LTG-01 well with the UHM-02 well (Figure 8-10). The well penetrated at the base clastics of Upper Devonian Famennian age (Van Hulten and Poty, 2009), but again this date cannot be confirmed, as biostratigraphic evidence is not presented.

Initial observations suggest that Luttelgeest platform is not founded on a structural high and the classic published lines show a relatively flat base and horizontal reflectors below.

However, other 2D lines suggest that there is indeed some structural character below, and it is likely that a fault-block high in the seeding point for carbonates.

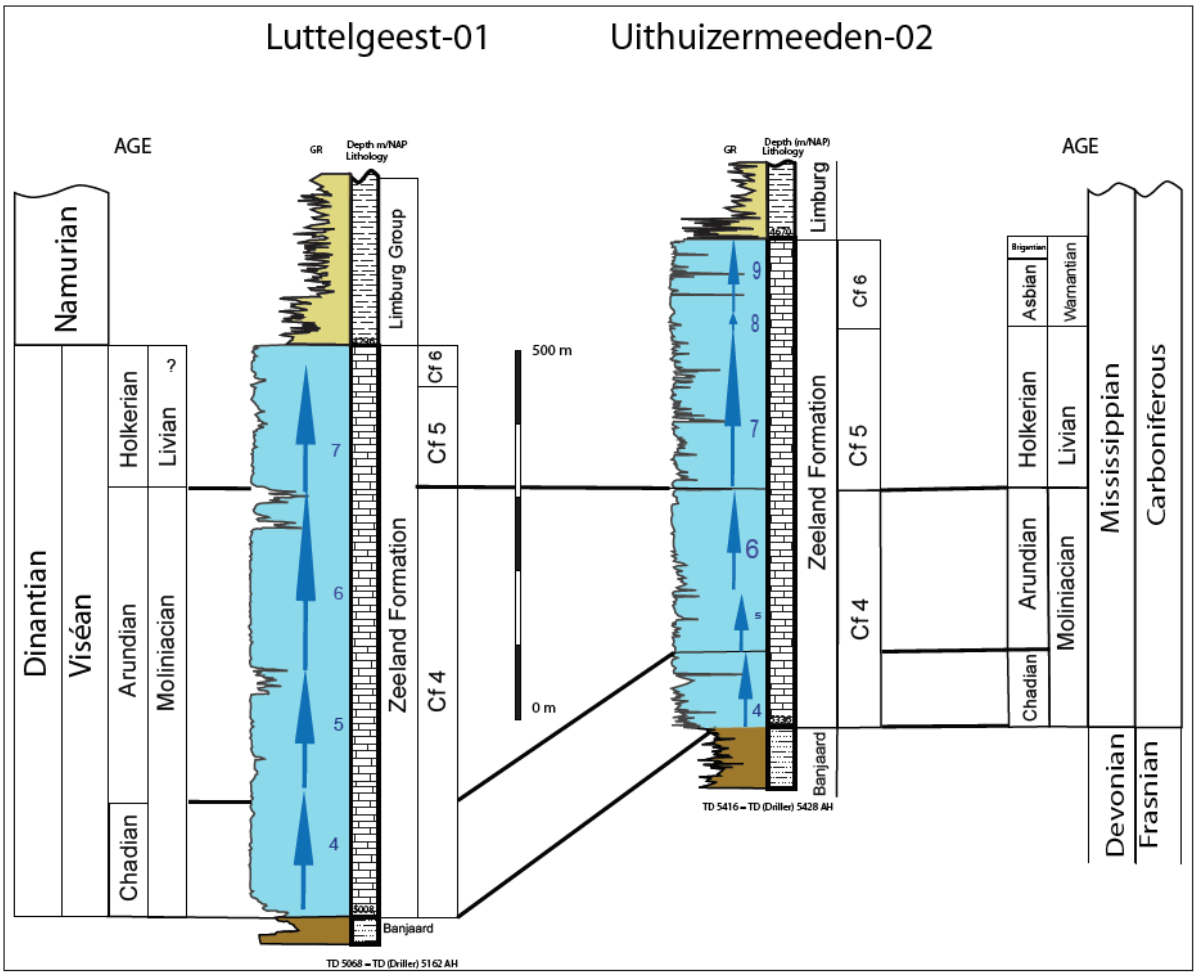

Figure 8-10: Correlation between the LTG-01 and UHM-02 wells (from Van Hulten, 2012).

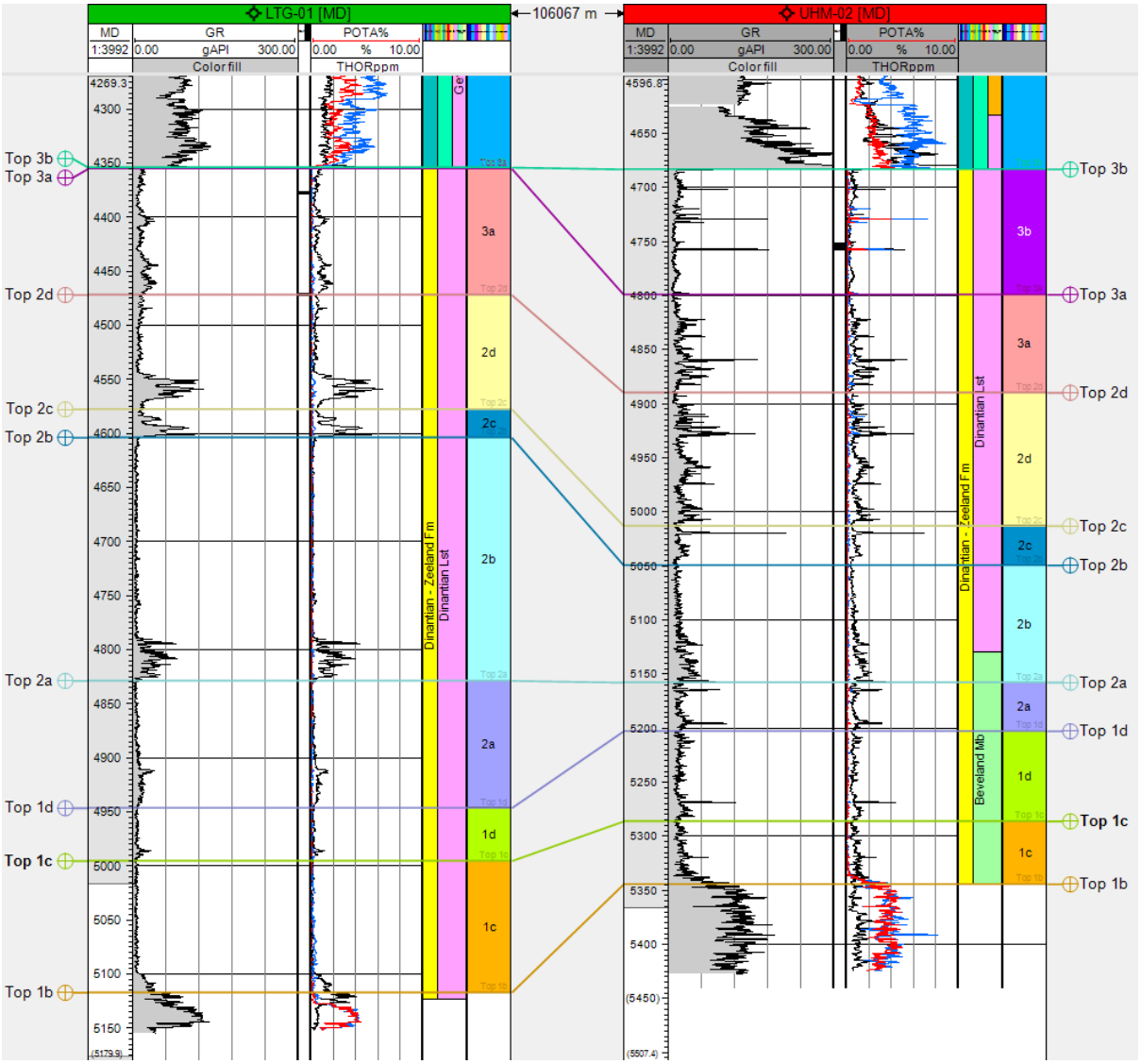

Figure 8-11: Depositional cycles and correlation between the LTG-01 and UHM-02 wells (SCAN project).

8.6 Sequence stratigraphy

The basal Dinantian sedimentary sequences recognised from the SW Netherlands are missing, and their absence is interpreted as a result of onlap of a structural high. The following depositional sequences have been tentatively recognised in the well (Figure 8-11):

Cycle 1c: This cycle represents the initial onlap of the basement high and itself is probably incomplete. The depositional setting was probably in a marginal mixed clastic-carbonate setting.

Cycle 1d: This cycle is a moderate gamma ray, thin TST followed by low gamma ray HST interpreted as a high energy platform interior depositional setting.

Cycle 2a: This cycle is a moderate gamma ray, broad TST followed by low gamma ray HST interpreted as a high energy platform interior depositional setting.

Cycle 2b: This cycle comprises a thick, high gamma ray TST to maximum flood, suggesting a period of drowning followed by thick very clean gamma ray HST interpreted as a high energy platform interior depositional setting.

Cycle 2c: This cycle is a thin depositional cycle consisting mainly of a high gamma ray TST and maximum flood followed by thin, moderate gamma ray HST interpreted as a low to moderate energy platform interior depositional setting.
Cycle 2d: This cycle has a thick, high gamma ray TST and maximum flood interpreted as a drowning event followed by thick clean gamma ray HST interpreted as a high energy aggradational platform interior depositional setting.
Cycle 3a: This cycle is interpreted as a platform interior setting. At least one flooding event may be present. Core information indicates deposition in a high energy carbonate platform interior setting above normal; wave base.

8.7 Diagenesis

Core observations indicate that diagenetic effects are rather limited in LTG-01. A key observation is the presence of two phases of fractures (Figure 8-12):

1. Relatively rare, sinuous/complex fractures that are subvertical to subhorizontal, and are cemented by calcite, and possible minor dolomite (orange colouration in part).
2. Subvertical fractures which are cemented by an initial calcite cement, and then locally a later dolomite cement. These post-date the earlier phase of fractures.

Small, calcite cemented vugs are also present, and may be early diagenetic in origin.
Patches of euhedral authigenic silica occur in the core, and are observed by hand lens. An interesting pyrite band is present at the top of core 2. This is approximately 10cm in thickness, and is cross cut by a set complex fracture set which is cemented by silica and another later phase of milky-white unknown mineral. It is unclear if the pyrite block is in place (i.e. whether it belongs to this well), as pyrite is not noted elsewhere.
The only other observations are of stylolites – these are postdated by subvertical fractures.

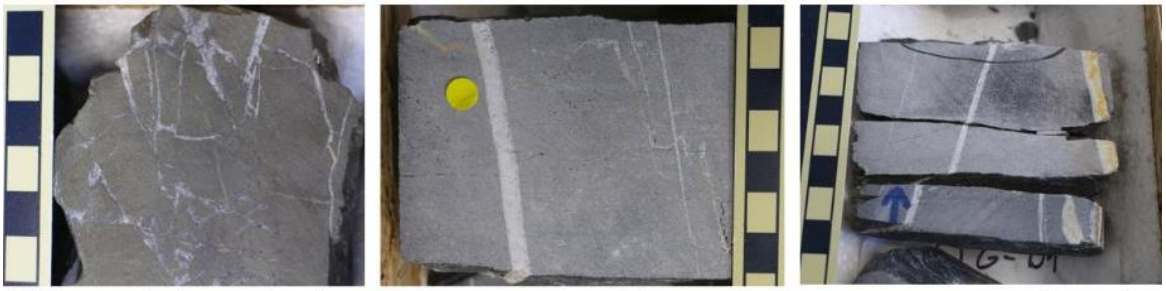

4470 m core 2. Fractured pyrite band

4472.10 m core 2. Calcite cemented fracture cross cutting complex sub-horizontal fracture

4470.62 m core 2. Calcite and dolomite cemented subvertical fracture.

Figure 8-12: Examples of cemented fractures (vein) in LTG-01.

8.7.1 Paragenetic sequence

Based on core and thin section observations, the following paragenesis is established (Figure 8-13). The representative images of the diagenetic phases are shown in Figures 8-14 to 8-18.

1. Early (marine?) calcite cement: C1 + (+ SC)
2. Dissolution and (meteoric) calcite cement (C2)
3. Equant calcite cement (occluding primary porosity) (C3)
3. Chemical compaction: stylolites
4. Fracturing and calcite cementation associated with HC, post-dating stylolites : C4
5. Fracturing (reactivation of calcite cemented veins) and saddle dolomite cementation + quartz:
   - SD1 + Q
   - SD2
   * locally replacive, non-saddle dolomite is observed, it is unclear if it is linked to the SD1 or SD2

→ Possible early meteoric dissolution and karstification, but most of the porosity is occluded by calcite cement (C3)

→Minor occurrence of saddle dolomite

Figure 8-13: Paragenetic sequences observed in the LTG-01 well.

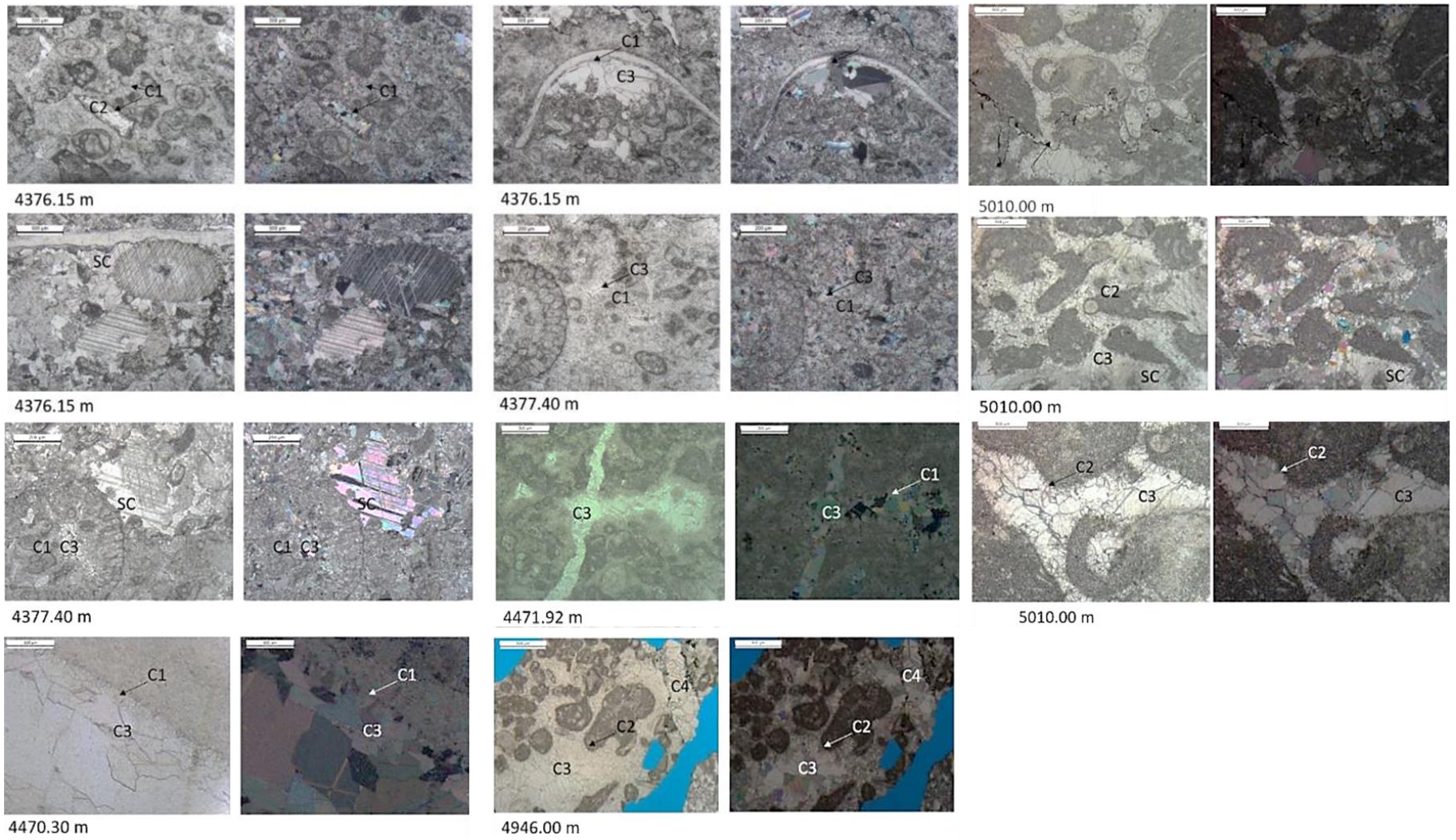

Figure 8-14: PPL and corresponding XPL images showing the types of calcite cements observed in LTG-01 thin sections. C1 is fine crystalline, fibrous, inclusion rich calcite (marine?). C2 is limpid dogtooth calcite (meteoric?). C3 is equant calcite (replacing aragonitic components and occluding primary porosity).

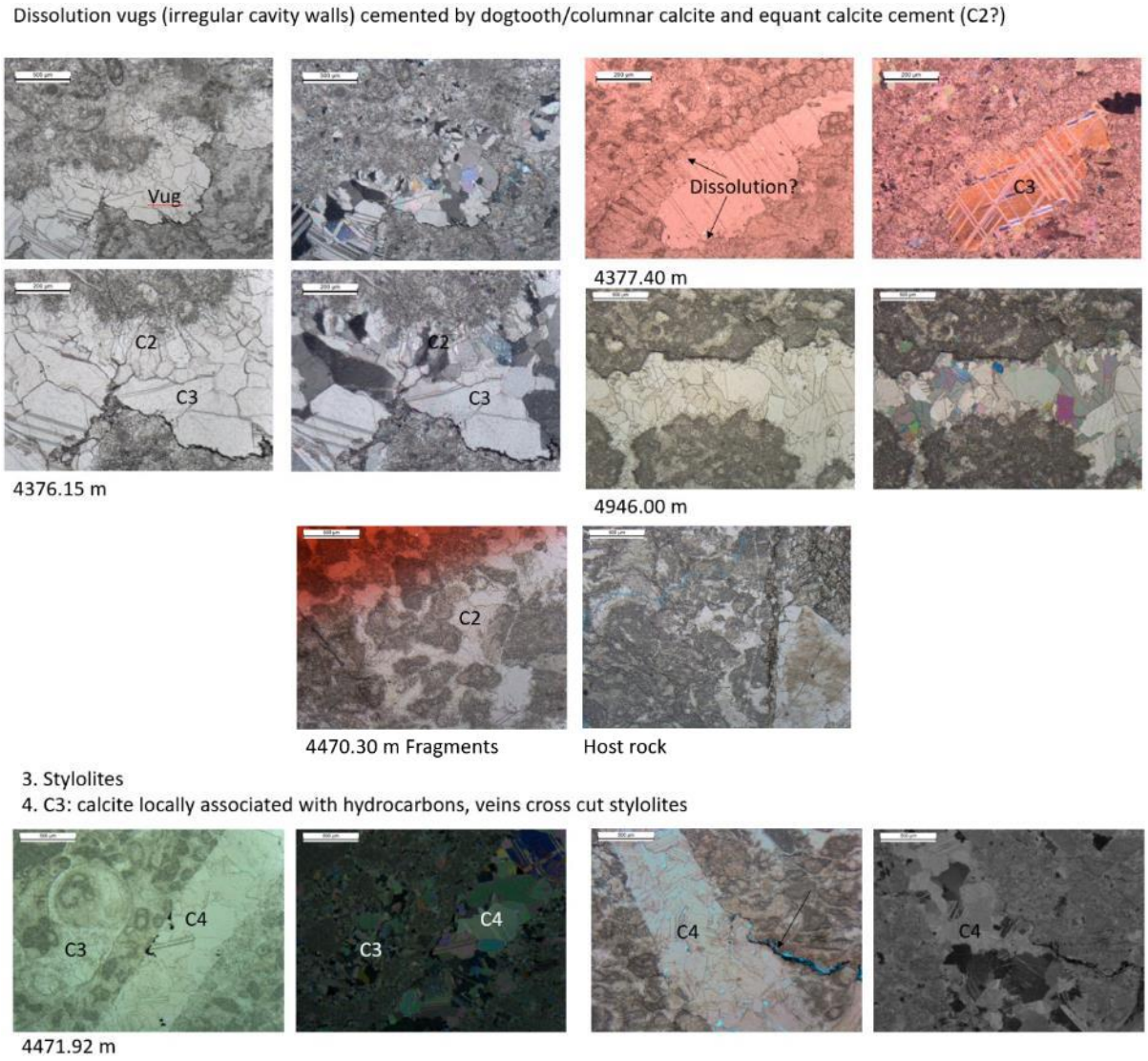

Figure 8-15: Photomicrographs showing the dissolution, vugs and calcite cements.

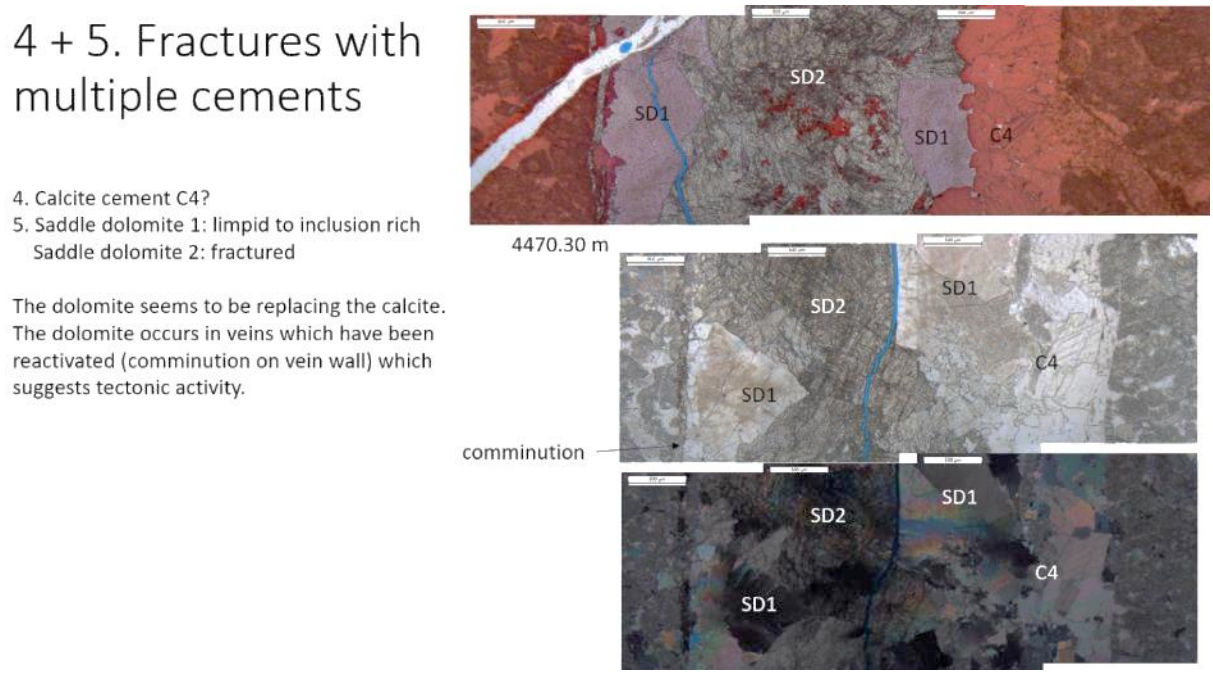

Figure 8-16: Fractures with multiple cements.

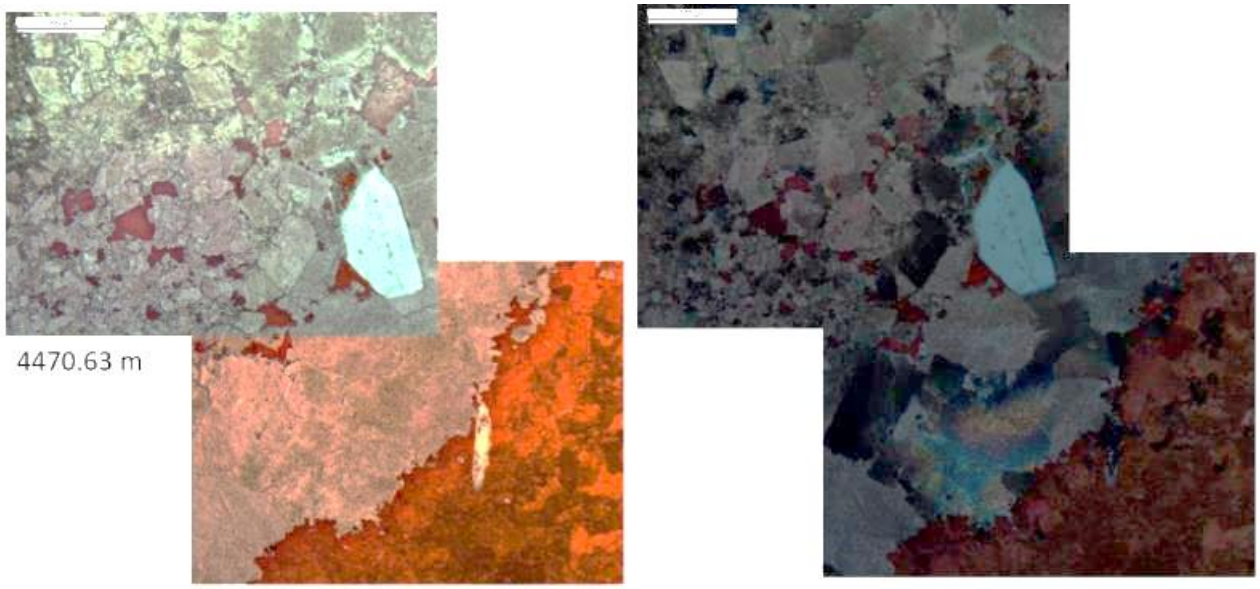

Figure 8-17: Quartz associated with dolomites (SD1).

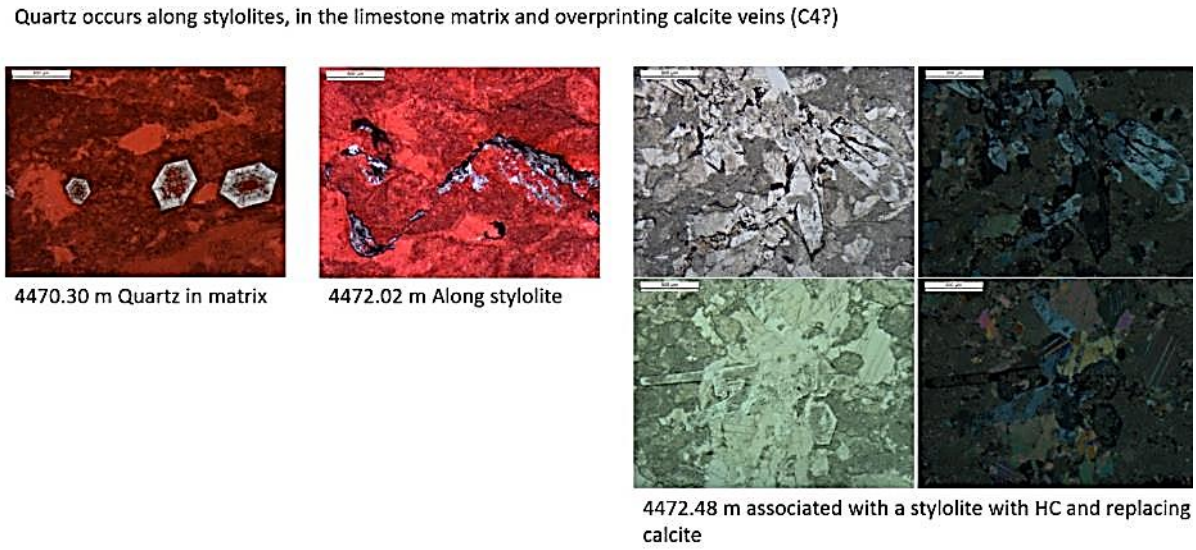

Figure 8-18: Quartz occurrences.

An early phase of fracturing may be associated with karstification, and there is evidence for early calcite cements being meteoric in origin (C2).
Based on Goldberg et al. (2017), commonly, fractures are filled with calcite spar. Some show enragement that may be due to karstification. Several factures contain an entire paragenetic series of carbonate minerals, the first being calcite spar (their C1) that possibly represents an early diagenetic phase of fracture and karstification. Calcite spar (C1) is succeeded by ferroan calcite/dolomite (FC/D). The differentiation was difficult due to dual carbonate staining. Contemporaneously and successively with FC/D baroque dolomite (SD) was formed within the factures. The saddle dolomite represents a later diagenetic phase with temperatures of at least 60 degrees and most likely much higher. The only porosity that was encountered in thin sections was intercrystalline porosity within dolomite SD. A very late generation of calcite (C2) occluded some of the porosity that was created during dolomite (SD) formation. Baroque dolomite occurs not only in fractures but also as interparticle cement. Absolutely no primary interparticle porosity was observed.
Stylolites occur very frequently, both as sutured contacts between grains as well as denticular stylolites. They formed pre- and post- calcite (C1). The stylolites are features of chemical compaction as a response to mechanical compaction of the carbonates. Authigenic euhedral quartz often occurs within stylolites and is surrounded by organic matter. Some quartz crystals contain calcite inclusions and organics. It seems that the quartz was formed due to compaction via recrystallisation of siliciclastic material. Quartz also formed within calcite fractures and was emplaced later than the calcite spar fill. The quartz formed both pre- and post-calcite spar but before the dolomite cementation.
Pyrite could have formed in an early diagenetic stage (shortly after deposition) or at high temperatures from thermochemical sulphate reduction. However, classical features of thermochemical sulphate reduction, such as anhydrite, fluorite, galena, sphalerite and high H_2S content are missing. Pyrite was mostly found within clay fragments, possibly representing early diagenetic formation. Only traces of pyrite were found within the carbonate layers. It is of course possible that intervals with hydrothermal indicators were missed due to low-resolution sampling.
According to the composite log the dolomite level is situated between ~ 5000 and 5100 m. According to the cuttings analysis the lithology is a dolomitic limestone rather than a pure dolomite. It is quite evident that the dolomite is a late diagenetic dolomite, however the exact

formation temperature and depth requires stable isotope and as well as fluid inclusion microthermometry analysis. The dolomite level is most suitable for encountering matrix porosity and permeability. However, porosity increase has not been inferred from the petrophysical logs within the dolomite interval. Although neutron porosity increases the density log increases likewise in this interval. This, however, can be purely an effect of the higher density of dolomite (2.85 g/cm2) compared to calcite (2.72 g/cm2). The dolomite level does not correspond to the assumed predominantly fractured interval between 4550 and 4800, (as constrained from mud losses).

TNO (Goldberg et al., 2017) performed clumped isotope analyses on fractures from sample 4470.3 m. Results suggest both the host rock and the first fracture cement phase resulted in high temperature of 210 to 220 °C. It is evident that both calcite phases do not represent the crystallisation (= emplacement) temperature but most likely the current temperature that must have been present for several Million years (1 to 100 Ma). The clumped isotope temperature of these calcites is very close to the downhole temperature measurements that range from 186 to 203 °C. The discrepancy between the measured downhole temperatures and the clumped isotope temperature could be due to the clumped isotope measurements having an error of ± 10 °C (which can be improved with more measurements) and downhole temperature having a standard deviation of ± 5 to 10 °C (Bonté et al., 2012).

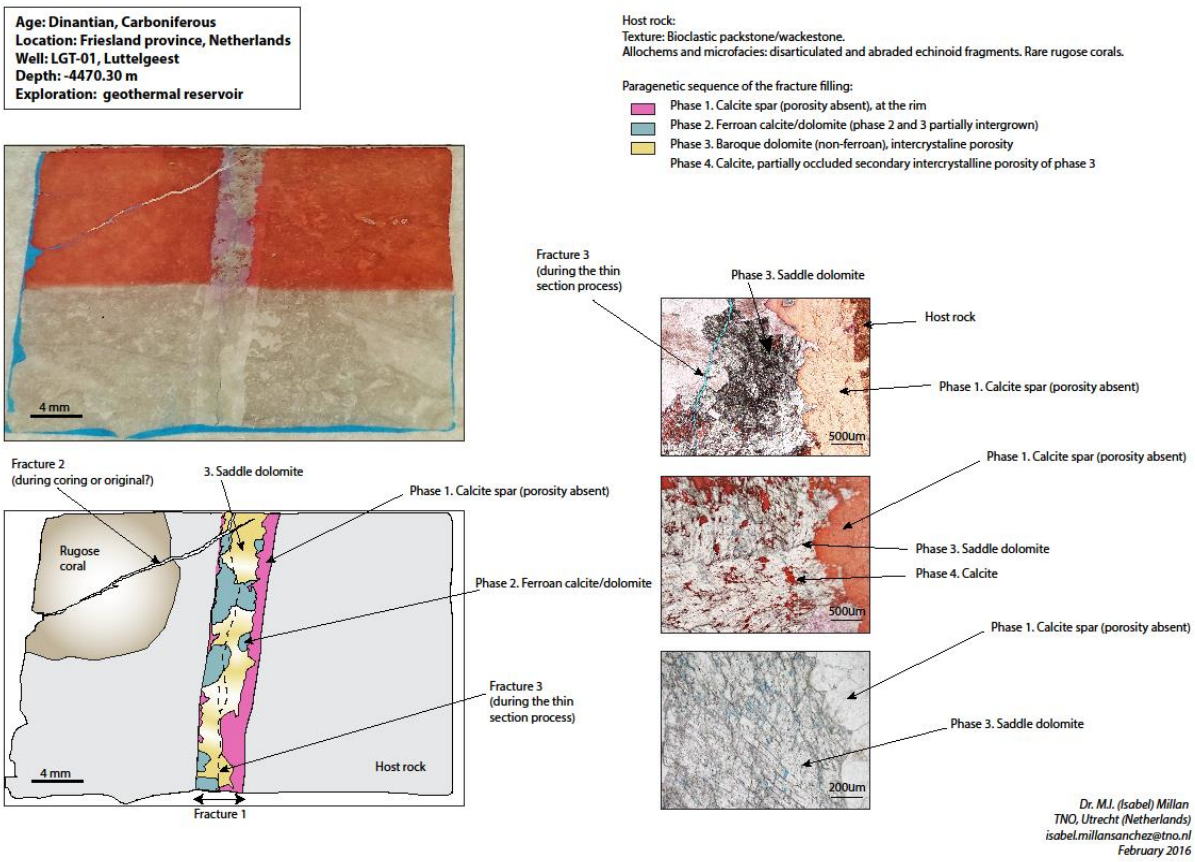

Figure 8-19: Different generations of calcite and dolomite cements are present in the fractures.

Table 8-5: Temperature estimations by using clumped isotopes analysis (from Goldberg et al., 2017).

Sample	Description	d13C VPDB	d18O VPDB	D47 CDES	Standard Error	D47 temperature °C	Standard Error
LGT-1 Bulk	bulk rock (not cemented)	1.74	-14.9	0.381	0.019	**220**	10
LGT-1 Cc Spar	Phase 1 cement	-1.43	-15.6	0.388	0.01	**210**	10
LGT-1 CCFe	Phase 2 cement	-1.68	-14.47	0.427	0.016	**167**	10
LGT-150 dolomite	Phase 3 cement	0.09	-13.87	0.657	0.012	**70**	10

Van Hulten and Poty (2009) found that fluid inclusion studies on core material were not conclusive but suggested that there may never have been methane trapped in the structure. The studies also indicated that temperatures have been at least 60 degrees higher than today (BHT abt. 200 °C).

8.8 Reservoir quality

The reservoir quality in the well as determined from core plugs is poor. Matrix porosity is below 2%. Permeability ranges from 0.2 to 9.6 mD. However, the core analyst noted that the higher measurements may be artifacts of a fractured core plug. Cuttings analysis suggest that dolomites may possess some intercrystalline porosity.

FMI logs were available for this project and were interpreted by Panterra, of which a detailed description is published in a separate report (Van Leverink and Geel, 2019). More than 900 fractures were identified in the well, with an average fracture density of 1.2 per meter. Several fracture clusters (or swarms) were identified. In a previous analysis, Van Hulten and Poty (2009) interpreted only a few fracture zones on the FMI. Two of these correspond with gamma ray peaks and were interpreted by van Hulten and Poty (2009) as karstification horizons.

Oversteeg et al. (2014) suggested intervals showing signs of fracture permeability range from 4550 to 5150 m measured depth. Several mud losses were encountered in well LTG-01; one at 4450 m, six between 4575 and 4700 m, one at 4775 and two between 4975 and 5025 m, which points to permeable zones that may be related to these fractures (Goldberg et al., 2017).

In-house petrophysics suggests porous zones around 4500 m, 4580 m, 4770 m, and 5000 m – these appear to tie-in with zones of dolomitisation.

Goldberg et al. (2017) made an attempt to estimate permeabilities from MDT measurements. TOTAL derived mobilities from the interpretation of MDT wireline pressures tests (Table 8.6). Out of the six measurements, three were found to be useable, i.e. not tight or supercharged. In order to derive permeabilities from mobilities, the fluid viscosities must be known. Goldberg et al. (2017) used an average mud viscosity of 95 centipoise. The calculated permeabilities for the useable measurements ranged from 126 to 598 mD. However, it can be questioned whether the choice of 95 centipoise is a valid one. If the seal of the MDT probe is intact, the liquid produced from the formation (either small fractures or pores) will be formation water and mud filtrate, and not the drilling mud. The used mud filtrate has a viscosity similar to a brine of 10,000 ppm salinity and 180 °C, which is around 0.2 cp instead of 95 cp, yielding permeabilities 500 times smaller than Table 8.6 suggests, i.e. from 0.28 to 1.26 mD.

Well testing recovered poor pressure data (Van Hulten and Poty, 2009). Tests did not recover any hydrocarbons. There were only slight gas shows from the mud log. Mud logging hardly recovered more methane than can be expected from background noise.

Table 8.6: Pressure tests and mobility values from wireline pressure measurements from Total. Permeability values calculated assuming mud viscosity or mud filtrate viscosity .

Depth [mAH]	Formation Pressure [Bar]	Remarks	Mobility [mD/cp]	Permeability [Md] Mud, 95 cp	Permeability [Md] Mud Filtrate, 0.2 cp
4445.6	613.2	Single probe. Tight/Supercharged	0.1		
4529.6	629.6	Single probe. Questionable	0.5		
4604.1	602.25	Single probe. Fair value	2.2	198	0.44
4604.5	602.66	Single probe. Fair value	1.4	126	0.28
4604.7	605.2	Dual probe. Good value	6.3	567	1.26
4646.8	604.5	Single probe. Supercharged	0.2		

This page intentionally left blank

Daalsesingel 1
3511 SV Utrecht
scan@ebn.nl
www.scanaardwarmte.nl

Onderzoek in de ondergrond voor aardwarmte